On-line analysis of free-tropospheric water-soluble acidic gases and particulate anions on the summit of Mt. Fuji, Japan

Masaki Takeuchi[a,b*], Naoya Tomiyasu[b], Makoto Namikawa[b], Hideji Tanaka[a,b], Kei Toda[c,d,e], Naoya Katsumi[f], Hiroshi Okochi[g]

[a] *Graduate School of Biomedical Sciences, Tokushima University, 1-78-1 Shomachi, Tokushima 770-8505, Japan*
[b] *Faculty of Pharmaceutical Sciences, Tokushima University, 1-78-1 Shomachi, Tokushima 770-8505, Japan*
[c] *Department of Chemistry, Kumamoto University, 2-39-1 Kurokami, Kumamoto 860-8555, Japan*
[d] *International Research Organization for Advanced Science and Technology, Kumamoto University, 2-39-1 Kurokami, Kumamoto 860-8555, Japan*
[e] *International Research Center for Agricultural and Environmental Biology, Kumamoto University, 2-39-1 Kurokami, Kumamoto 860-8555, Japan*
[f] *Faculty of Bioresources and Environmental Sciences, Ishikawa Prefectural University, 1-308 Suematus, Nonoichi, Ishikawa 921-8836, Japan*
[g] *Department of Resources and Environmental Engineering, Waseda University, 3-4-1 Okubo, Shinjuku-ku, Tokyo 169-8555, Japan*

[*] Corresponding author.
E-mail: masaki.takeuchi@tokushima-u.ac.jp

Abstract

Atmospheric gaseous and particulate pollutants emitted from local or regional sources cause transboundary air pollution. To better understand this environmental issue, it is useful to monitor the free troposphere, reflecting the global air quality, with high temporal resolution. During the summer of 2016, we operated an original on-line monitor on the summit of Mt. Fuji, Japan (3776 m a.s.l.) to measure water-soluble acidic gases and particulate anions in the free troposphere. Mt. Fuji is a free-standing mountain and, therefore, hardly affected by air pollutants emitted from the local region. The lab-made gas/particle collector coupled ion chromatograph successfully provided meaningful data on an hourly basis. The average concentrations of HNO_3, SO_2, NO_3^-, and SO_4^{2-} (n = 64 each) were, respectively 1.8 ± 0.9, 2.3 ± 2.5, 0.22 ± 0.16, and 3.9 ± 2.6 nmol m^{-3}. The gaseous HNO_3 was the predominant form compared to particulate NO_3^-. For the sulfur component, the percentage of particulate form was higher than that of the gaseous one. The high time-resolution monitoring enabled us to classify the observed data based on the air parcel inflow direction to the sampling point even when it changed dramatically. As a result, the oxidation of SO_2 to SO_4^{2-} in atmospheric transport can be discussed for each air parcel. It was suggested that the SO_2 oxidation was enhanced in the air parcels that passed over the Asian Continent.

Keywords: Acidic gases, Particulate anions, Free troposphere, High-time resolution, Free-standing mountain.

1. Introduction

The chemistry of the free troposphere reflects the global air quality rather than the planetary boundary layer, which is more influenced by the local air pollutions (Camarero, 2017). Ground-based observations at high-altitude mountain sites provide background trace gases and particles in the free troposphere (Okamoto and Tanimoto, 2016). Mt. Fuji, the highest mountain in Japan, is a free-standing mountain (stand-alone mountain that is not a part of any mountain range), the summit (3776 m a.s.l.) located in the free troposphere. Anthropogenic air pollutants emitted from the Asian continent are transported over Japan by westerly winds (Igarashi et al., 2010). Therefore, the summit of Mt. Fuji is a preferred platform to monitor the long-range transport of air pollutants and the background level of atmospheric composition over Japan. Air pollution is caused by a complex mixture of thousands of components. The variety includes atmospheric particulate matter and gaseous pollutants such as sulfur dioxide (SO_2) and nitrogen oxides (NO_x). These air pollutants are not only destructive to the natural environment, but increase the risk of respiratory, cardiovascular, and other diseases (Newby et al., 2015). SO_2 is the predominant anthropogenic air pollutant and is emitted directly into the atmosphere by combusting fossil fuels containing sulfur (Seinfeld and Pandis, 1998). NO_x emitted directly from automobiles, power plants, and factories is oxidized to nitric acid (HNO_3) in the atmosphere (Kitto and Harrison, 1992; Streets and Waldhoff, 2000). Together with volatile organic compounds and ammonia, these acidic gases are the main precursors of secondary particulate matter (Finlayson-Pitts and Pitts, 1999). Depending on the region, 60-70% of the particulate matter in the atmosphere is water-soluble, principally nitrate (NO_3^-) and sulfate (SO_4^{2-}) (Warneck, 1999).

Filter pack methods are widely applied to the collection of water-soluble trace gases/particles in the atmosphere (Finlayson-Pitts and Pitts, 1999). The filter-based methods are simple but require a time-consuming process, i.e., off-line extraction, filtration, and analysis by ion chromatography (Takeuchi et al., 2004b). In addition, the off-line approaches cannot provide the high-time resolution data that helps to study the transboundary transport of atmospheric chemicals and pollutants. For 12-hour or 24-hour off-line measurements, the air parcel trajectory may change significantly during the sampling. Diffusion scrubber/denuder techniques (Takeuchi et al., 2004a; Takeuchi et al., 2013; Ullah et al., 2006) or continuous particle collectors (Al-Horr et al., 2003; Takeuchi et al., 2005; Mitsuishi et al., 2018) coupled ion chromatographic systems can provide higher temporal resolution and more accurate observation results. We monitored the free-tropospheric HNO_3 and SO_2 at the summit of Mt. Fuji (Takeuchi et al., 2017), using a parallel-plate wet denuder coupled ion chromatograph (PPWD-IC) (Boring et al., 2002; Takeuchi et al., 2011) and revealed the daily behaviors of the acidic gases. On the other hand, the particles corresponding to HNO_3 and SO_2, particulate NO_3^- and SO_4^{2-}, exist in the free troposphere, and the existence phase of these reactive substances varies rapidly with meteorological conditions. Therefore, simultaneous measurement of HNO_3, SO_2, NO_3^-, and SO_4^{2-} is desired to clarify air pollutants' behavior in the free troposphere. However, as far as we know, no one has successfully measured the free-tropospheric particulate anions with a high time-resolution due to various difficulties during observations.

In the summer of 2016, we wrestled with the simultaneous detection of the free-tropospheric acidic gases (HNO_3, SO_2) and particulate anions (NO_3^-, SO_4^{2-}) with one-hour resolution on the summit of Mt. Fuji. Incorporating a hydrophobic filter/mist chamber-based particle collector (PC) (Al-Horr et al., 2003; Takeuchi et al., 2012) into the PPWD-IC, the gaseous and particulate components were continuously measured with a single ion chromatographic system. In the present paper, we revealed temporal variations of the free-tropospheric particulate NO_3^- and SO_4^{2-} as well as their precursors SO_2 and HNO_3 for the first time. The data obtained allowed us to study the influence of local air pollutants on the free troposphere air sampled, which is a significant concern for atmospheric observation at high-altitude mountain sites. In addition, the high time-resolution data enabled us to precisely classify the observed values by the direction of air parcel inflow. As a result, the concentration levels of transboundary polluted air and background trace gases and particles in the global air can be more accurately represented.

2. Methods

2.1. Reagents and chromatographic system

All reagents used in the present study were of analytical grade and were used without further purification. Sodium nitrate and sodium sulfate were purchased from Kanto Chemical Co. Inc. Hydrogen peroxide was purchased from Mitsubishi Gas Chemical Co., Inc. Sartorius arium 611DI grade deionized water (>18 MΩ cm) was used throughout.

An ICS-2100 ion chromatograph was used with an IonPac ATC-HC anion trap column, an EGC III KOH eluent generator cartridge, an IonPac AG20 2-mm guard column, an IonPac AS20 2-mm separation column, an ASRS300 2-mm electrodialytic suppressor, a CRD200 2-mm carbonate removal device, and a DS6 heated conductivity detector. Instead of a sample loop, an IonPac TAC-ULP1 anion preconcentrator column was connected to a 6-port injector. An 8 mmol L^{-1} KOH eluent was used isocratically at a flow rate of 0.20 mL min^{-1}. The suppressor operated at 5 mA of current with recycle mode. The guard/separation columns and conductivity cell were maintained at 30°C. The chromatographic system was calibrated by injecting mixed-standard nitrate and sulfate solutions. Acquisition of the detector signals and system control were carried out under software control (Chromeleon Ver. 6.8). All of the chromatographic hardware and software described above were purchased from Thermo Fisher Scientific Inc.

2.2. Gas and particle collectors

A lab-made PPWD was used for the continuous collection of water-soluble gases. Details of the PPWD have been described previously (Boring et al., 2002; Takeuchi et al., 2011). In short, the PPWD was composed of two Plexiglas plates and a Teflon spacer. The inner surfaces of the end plates (42 cm

length, 6 cm width, 0.3 cm distance) were microstructured to improve the wettability with a denuder liquid. The denuder liquid was pumped to flow down each plate and was aspirated from the bottom. Meanwhile, the sample air entered at the bottom of the PPWD and flowed into space between the end plates. The PPWD quantitatively collects water-soluble acidic gases at a sampling flow rate of 3 to 10 L min^{-1} (Takeuchi et al., 2011). The potential interference with 0 – 250 parts per billion by volume (ppbv) NO and 0 – 80 ppbv NO_2 on the measured value of HNO_3 is less than 0.06% (total moles basis) in the worst case (Simon and Dasgupta, 1995).

A particle collector, PC, used for continuous collection of the atmospheric particulate matter, was also lab-made (Al-Horr et al., 2003; Takeuchi et al., 2012). Briefly, the PC consisted of an air/liquid nozzle, a cylindrical mist chamber (6.4 cm i.d., 9.5 cm height), and an air/liquid separator. The sample air passed through the PPWD entered the mist chamber through a tapered Plexiglas nozzle (1.0 mm terminal orifice). The PC liquid was pumped to the air stream just exiting the air nozzle. High-velocity air created a fine liquid mist in the chamber. The particles captured by the PC liquid were aspirated from a liquid outlet aperture on the bottom. A hydrophobic microporous PTFE membrane filter (Fluoropore membrane filter, 0.45 mm pores, 47 mm dia., Millipore Corp.) at the top of PC provided the air exit. The PC quantitatively collects the particle with mass median aerodynamic diameter from 0.21 to 7.8 μm at sampling flow rates of at least up to 6 L min^{-1} (Al-Horr et al., 2003).

2.3. Gas/particle monitoring system

The overall air/liquid flow arrangement of the gas/particle monitoring system is illustrated in Fig. 1. The air sample was aspirated by a diaphragm vacuum air pump (model doA-P501-DB, Gast Manufacturing Inc.) through a water trap (Balston disposable filter unit, 9900-05-BK, Parker Hannifin Corp.). It was controlled at 3.0 standard liters per minute (SLPM) with a mass flow controller (Model 8500, Kofloc Co. Ltd.). A 2 m of PFA Teflon tube (3.96 mm i.d., 6.35 mm o.d.) was used as the air inlet. A 0.5 mmol L^{-1} hydrogen peroxide as the denuder liquid was delivered to the PPWD at 0.25 mL min^{-1} $plate^{-1}$ by a peristaltic pump (RP-1, Rainin Instrument Co.). As the PC liquid, deionized water was pumped to the PC at 0.45 mL min^{-1}. Before collecting gas/particles, any undesirable ions in both the liquids were removed with anion trap columns (ATC3 9-mm, Thermo Fisher Scientific Inc.). The PPWD/PC's effluents were continuously delivered to each 50-mL polypropylene tube (CELLMASTER, Greiner Bio One International GmbH) at > 0.5 mL min^{-1}. One of the liquid samples was then aspirated to the anion preconcentrator column via a 3-port valve (3 ports of a Valco Instruments Co. Inc. Cheminert C2 10-port high-pressure valve were used) that was switched to the other position at 30 min intervals. At the end of 25 min sample loading to the anion concentrator, a 6-port valve was switched to injection mode for 5 min. The analyte was determined utilizing ion chromatography. This gas/particle monitoring system automatically provides the data for acidic gases and particulate anions every hour as 28 min average concentration. The limits of detection, LODs, calculated by $3\sigma/S$, where σ and S are the residual standard deviation and slope of the regression line were 0.00075

nmol m^{-3} for gaseous HNO_3, 0.023 nmol m^{-3} for SO_2, 0.00075 nmol m^{-3} for particulate NO_3^-, and 0.021 nmol m^{-3} for SO_4^{2-}, respectively.

2.4. Monitoring period and monitoring site

The gas/particle monitoring system was set up in the Mount Fuji Research Station (MFRS, formerly known as Mt. Fuji Weather Station) located at the summit of Mt. Fuji (35.36°N, 138.73°E, 3776 m a.s.l.), Japan. The system was continuously operated from July 10 to 12 in 2016. Mt. Fuji is a free-standing mountain, and the summit of which is beyond a tree line.

2.5. Meteorological conditions

The Japan Meteorological Agency provided hourly averaged air temperature and relative humidity at the summit. The National Astronomical Observatory of Japan provided the data of sunrise and sunset. Three-day backward trajectories of air parcels reaching the summit were calculated using the NOAA HYSPLT 4 model. A meteorological data set was used for GDAS and model vertical velocity data for vertical motion. The initial elevation reading by the trajectory analysis was 3776 m.

3. Results and discussion

3.1. Concentration levels of free-tropospheric HNO_3, SO_2, NO_3^-, and SO_4^{2-}

During the summer campaign in 2016, the gas/particle monitoring system has successfully operated without any maintenance and provided meaningful data for acidic gases (HNO_3, SO_2) and particulate anions (NO_3^-, SO_4^{2-}) every hour. The average temperature, relative humidity, and barometric pressure were 5.6 ± 1.2°C, 55 ± 28%, and 645.0 ± 0.5 hPa, respectively, and there was no rainfall during the campaign. Note that the gas and particle concentrations data in the present study are corrected to nmol m^{-3} at 5.6°C and 645.0 hPa, and the average data are expressed as mean ± one standard deviation. The average and median acidic gas concentrations (n = 64 each) were, respectively, 1.8 ± 0.9 nmol m^{-3} and 1.6 nmol m^{-3} for HNO_3, 2.3 ± 2.5 nmol m^{-3} and 1.4 nmol m^{-3} for SO_2. These concentration levels are comparable to the average concentrations obtained from the 2012 summer campaign at the summit of Mt. Fuji (0.86 ± 0.55 nmol m^{-3} for HNO_3, 1.7 ± 2.0 nmol m^{-3} for SO_2, n = 672 each, Takeuchi et al., 2017). Besides, a few studies have so far been reported the average concentration of SO_2 at the summit of Mt. Fuji, *e.g.,* 1.9 nmol m^{-3} for July 26-August 3 in 1993 and 0.7 nmol m^{-3} for July 26-30 in 1994 (Dokiya et al., 1995), 1.4 nmol m^{-3} for July 2003 (Igarashi et al., 2004). Kato et al. (2016) reported high concentrations of SO_2 at the summit of Mt. Fuji on August 20-21, 2013, although there is no description of the averaged SO_2 level. The concentrations of HNO_3 and SO_2 at the summit of Mt. Fuji shown here

are one order of magnitude lower than those in urban areas, *e.g.*, Tokushima, Japan (midsized city): 18.6 nmol m^{-3} HNO_3 and 50.3 nmol m^{-3} SO_2 for August 2011 (Takeuchi et al., 2013).

There have been no reports available on the particulate anions monitored with a good time resolution at the summit of Mt. Fuji. The average and median anion concentration in the particulate matter observed in the present study (n = 64 each) were, respectively, 0.22 ± 0.16 nmol m^{-3} and 0.22 nmol m^{-3} for NO_3^-, 3.9 ± 2.6 nmol m^{-3} and 3.0 nmol m^{-3} for SO_4^{2-}. The average and median concentrations of SO_4^{2-} were an order of magnitude higher than those of NO_3^-, the ratio of the average and median concentration of SO_4^{2-} to NO_3^- (S/N) being 18 and 14, respectively. Suzuki et al. (2008) collected atmospheric particulate matter at the summit of Mt. Fuji using a high-volume air sampler and reported a similar S/N to our observation. They found that the sample volume-weighted average concentrations during summers in 2001 and 2002 were 1.2 nmol m^{-3} for NO_3^- and 15.3 nmol m^{-3} for SO_4^{2-} (S/N = 13). On July 28-August 2 in 1993, Tsuboi et al. (1996) also sampled particulate NO_3^- and SO_4^{2-} at the summit of Mt. Fuji using a low volume air sampler with the time resolution 4 h. They reported that the detected SO_4^{2-} levels were significantly higher than the NO_3^-, while approximately half for NO_3^- and one-third for SO_4^{2-} the total samples were below the detection limits. Several studies using filter-based off-line approaches have revealed anions concentration in the particulate matter at other high-altitude mountain sites, *e.g.,* Mt. Sonnblic (3106 m a.s.l.): 2.2 nmol m^{-3} NO_3^- and 17.4 nmol m^{-3} SO_4^{2-} for July 1992 (Kasper and Puxbaum, 1998), Jungfraujoch (3580 m a.s.l): 5.3 nmol m^{-3} NO_3^- and 7.1 nmol m^{-3} SO_4^{2-} for summers in 1999 and 2000 (Henning et al., 2003), Mont Blanc massif (4360 m a.s.l.): 2.1 nmol m^{-3} NO_3^- and 6.5 nmol m^{-3} SO_4^{2-} for September 2004 (Preunkert et al., 2007). Note that these are a part of the mountain range rather than a free-standing mountain like Mt. Fuji. The concentration levels of particulate NO_3^- and SO_4^{2-} at European mountain sites mentioned above are higher than those observed in the present study.

3.2. Time variations of HNO_3, SO_2, NO_3^-, and SO_4^{2-} concentrations at the summit of Mt. Fuji

Whether or not the free-tropospheric air is sampled, i.e., local air pollutants have little influence on the concentration levels observed, is of significant concern for the atmospheric observation at high-altitude mountain sites. Mt. Fuji is a free-standing mountain located in the free troposphere and is considered hardly influenced by local pollutions. Previous studies have suggested that local air in the planetary boundary layer (PBL) barely affects the concentrations of gaseous substances at the summit of Mt. Fuji (Nakazawa et al., 1984; Murosaki et al., 2006; Yokota et al., 2009). However, on the other hand, the influences of upward mixing of PBL air on the particulate matter concentration at the summit of Mt. Fuji have been pointed out. During summers in 1997 and 1999, Hayashi et al. (2001) obtained aerosol samples at the summit of Mt. Fuji with a time resolution of 4 h. They found the diurnal variation of particulate SO_4^{2-} concentration, i.e., the peaks during 12:00-16:00. They concluded that the local pollutants in PBL were transported to the summit by the valley wind blowing in the afternoon. Kaneyasu and Igarashi (2007) also revealed that the black carbon concentration at the summit of Mt. Fuji in early summer showed an obvious diurnal pattern with

daytime maxima and morning minima. Our gas/particle monitoring system allows simultaneous monitoring of acidic gases and particulate anions every hour. Therefore, it is possible to determine diurnal cycles and investigate how much the PBL influences the concentration levels of air at the summit. Fig. 2 presents the temporal variations of atmospheric HNO_3, SO_2, NO_3^-, and SO_4^{2-} concentrations at the summit of Mt. Fuji along with the meteorological data. The acidic gas concentrations and particulate SO_4^{2-} and NO_3^- did not show a distinct shift even though each concentration fluctuated in a short time. The daytime/nighttime concentrations ratio was mostly around one (HNO_3: 0.96, SO_4^{2-}: 1.14, and NO_3^-: 0.90) except SO_2 (1.56). Therefore, the present study's concentration levels might be less influenced by the upward mixing of PBL air.

In our previous high time-resolution observations of atmospheric HNO_3 and NO_3^- in the PBL, the molar ratio of HNO_3 to total NO_3 (sum of HNO_3 and NO_3^-) varied below 50% (Takeuchi et al., 2017; 2021). Meanwhile, the gaseous HNO_3 was the predominant form compared to particulate NO_3^- during the present campaign, as shown in Fig. 2. The molar ratio of HNO_3 to total NO_3 varied from 60.2 to 99.6%, with an average of 86.4 ± 10.0%. The HNO_3 formed, and present at high altitudes might be limited in its conversion to particulate NO_3^-. Such a trend in increasing HNO_3 fraction has been observed at other sampling sites. Dibb et al. (2003) reported that the mass ratio of atmospheric HNO_3 to total NO_3 increased with pressure altitude (e.g., 50% at 0.7 km, 70% at 3.5 km, 95% at 10.5 km). Huebert and Lazrus (1978; 1980) found that the molar ratios of HNO_3 vapor to particulate NO_3^- were always greater than unity above the PBL.

The molar ratio of SO_2 to total SO_4 (sum of SO_2 and SO_4^{2-}) averaged 35.1% but varied considerably from 10.1 to 84.5% hourly. The changes in meteorological conditions are expected to promote the particulation of SO_2. However, the correlation analysis showed no significant correlation between the molar ratio of SO_2 to total SO_4 and the meteorological conditions (temperature, relative humidity). Therefore, in the next section, we decided to use a backward-trajectory analysis to clarify the relationship between the present form of sulfur species and the air parcel that reached the sampling site.

3.3 Back-trajectory analysis

Fig. 3 shows the three-day backward trajectories of air parcels reaching the summit of Mt. Fuji during the summer campaign. The backward trajectory analysis showed that the air parcels could be roughly divided into three categories: A, via the Sea of Japan (27% frequency); B, via Russia, northeastern China, and via the Korean Peninsula (48%), and C, via the East China Sea (25%). During the campaign, the direction of air parcel inflow changed from A to C over time. The high time-resolution data obtained in the present study enabled us to classify the observed values by the direction of air parcel inflow even when the movement of air parcel inflow changed significantly within 24 hours.

Fig. 4 shows the average concentrations of acidic gases and particulate anions classified according to the air parcel trajectory pattern. The air parcel C that had passed over the East China Sea contained

low levels of pollutants (0.84 nmol m^{-3} for HNO_3, 1.0 nmol m^{-3} for SO_2, 0.24 nmol m^{-3} for NO_3^-, 1.9 nmol m^{-3} for SO_4^{2-}) than the other air parcels. The SO_4^{2-} is recognized as a major particulate component in transboundary air pollution over East Asia (Kaneyasu et al., 2014). The high SO_2 and SO_4^{2-} levels were transported from Asian Continent to Japan (Itahashi and Hayami, 2015). Therefore, we evaluated the behaviors of SO_2 and SO_4^{2-} based on the air parcel C. Table 1 provides the ratios of SO_4^{2-} to sum of SO_4^{2-} and NO_3^- concentration, SO_2 to the sum of SO_2 and HNO_3 concentrations, and SO_4^{2-} to SO_2 concentration for each air parcel. The ratio of SO_4^{2-} concentration to the sum of SO_4^{2-} and NO_3^- concentrations were high in the air parcels A and B, suggesting the long-range transport of air pollutants. Meanwhile, the ratio of SO_2 concentration to the sum of SO_2 and HNO_3 concentrations was high in air parcel A but low in B. Since the ratio of SO_4^{2-} to SO_2 concentration is high in air parcel B, the oxidation rate of SO_2 to SO_4^{2-} would be high. The air parcel B passed over the Asian Continent, where there might be an abundance of oxidants such as ozone and hydroxyl radicals in the atmosphere. Therefore, the relatively low ratio of SO_2 to the sum of SO_2 and HNO_3 concentrations for the air parcel B is probably due to the accelerated oxidation of SO_2 to SO_4^{2-} in the transport process.

4. Conclusions

In the summer campaign of 2016, simultaneous measurement of HNO_3, SO_2, NO_3^-, and SO_4^{2-} in the free troposphere with high time-resolution was successfully achieved at the summit of Mt. Fuji, Japan. The gas/particle monitoring system, consisting of a lab-made parallel plate wet denuder, hydrophobic filter/mist chamber-based particle collector, and ion chromatograph, automatically provided valuable data on the acidic gases and particulate anions on an hourly basis. The average acidic gas and particulate anions concentrations were, respectively, 1.8 ± 0.9 nmol m^{-3} for HNO_3, 2.3 ± 2.5 nmol m^{-3} for SO_2, 0.22 ± 0.16 nmol m^{-3} for NO_3^-, and 3.9 ± 2.6 nmol m^{-3} for SO_4^{2-}. The molar ratio of HNO_3 to total NO_3 varied from 60.2 to 99.6%, with an average of 86.4 ± 10.0%. Meanwhile, the molar ratio of SO_2 to total SO_4 averaged 35.1% but varied considerably from 10.1 to 84.5% hourly. The temporal variation data suggested that the concentration levels of acidic gases and particulate anions at the summit of Mt. Fuji are less sensitive to upward mixing of PBL air. Therefore, the observations of the free troposphere at the summit of Mt. Fuji are ideal for monitoring global air quality. In addition, the high time-resolution data effectively identified the sources of long-range transported air pollutants and helped investigate the oxidation of SO_2 to SO_4^{2-} during atmospheric transport. The air parcel that passed over the East China Sea was relatively clean, and its concentration levels (0.84 nmol m^{-3} for HNO_3, 1.0 nmol m^{-3} for SO_2, 0.24 nmol m^{-3} for NO_3^-, 1.9 nmol m^{-3} for SO_4^{2-}) would be the background level of the global air.

Acknowledgments

This work was performed during the period in which the Certified Nonprofit Organization Mount Fuji Research Station (MFRS) maintained the facilities and was partly supported by the Grant-in-Aid for Scientific Research(C) (26340006, 17K00521) from the Japan Society for the Promotion of Science, and the research program for the development of intelligent Tokushima Artificial Exosome (iTEX) from Tokushima University.

References

Al-Horr, R., Samanta, G., Dasgupta, P.K., 2003. A continuous analyzer for soluble anionic constituents and ammonium in atmospheric particulate matter. Environ. Sci. Technol. 37, 5711-5720.

Boring, C. B., Al-Horr, R., Genfa, Z., Dasgupta, P. K., Martin, M. W., Smith, W. F., 2002. Field measurement of acid gases and soluble anions in atmospheric particulate matter using a parallel plate wet denuder and an alternating filter-based automated analysis system. Anal. Chem. 74, 1256-1268.

Camarero, L., 2017. Atmospheric chemical loadings in the high mountain: Current forcing and legacy pollution. In: Catalan, J., Ninot, J., Aniz, M. (eds.) High mountain conservation in a changing world. Springer, Cham, Switzerland, pp 325-341.

Dibb, J. E., Talbot, R. W., Scheuer, E. M., Seid, G., Avery, M. A., Singh, H. B., 2003. Aerosol chemical composition in Asian continental outflow during the TRACE‐P campaign: Comparison with PEM‐West B. J. Geophys. Res. Atmos. 108, 8815.

Dokiya, Y., Tsuboi, K., Sekino, H., Hosomi, T., Igarashi, Y., Tanaka, S., (1995). Acid deposition at the summit of Mt. Fuji: Observations of gases, aerosols and precipitation in summer, 1993 and 1994. Water Air Soil Pollut. 85, 1967-1972.

Finlayson-Pitts, B. J., Pitts, J. N., Jr., 1999. Chemistry of the Upper and Lower Atmosphere: Theory, Experiments, and Applications. Academic Press, San Diego.

Hayashi, K., Igarashi, Y., Tsutsumi, Y., Dokiya, Y., 2001. Aerosol and precipitation chemistry during the summer at the summit of Mt. Fuji, Japan (3776 m a.s.l.). Water Air Soil Pollut. 130, 1667.

Henning, S., Weingartner, E., Schwikowski, M., Gäggeler, H., Gehrig, R., Hinz, K.-P., Trimborn, A., Spengler, B., Baltensperger, U., 2003. Seasonal variation of water-soluble ions of the aerosol at the high-alpine site Jungfraujoch (3580 m asl). J. Geophys. Res. 108, 4030.

Huebert, B., Lazrus, A. L.,1978. Global tropospheric measurements of nitric acid vapor and particulate nitrate. Geophys. Res. Lett. 5, 577-580.

Huebert, B., Lazrus, A. L., 1980. Tropospheric gas-phase and particulate nitrate measurements. J. Geophys. Res. 85, 7322-7328

Igarashi, Y., Naoe, H., Takahashi, H., Inomata, Y., 2010. Observation of atmospheric chemistry by using mountains, research trends and its challenges -a mini review. Low Temp. Sci. 68, 69-78.

Igarashi, Y., Sawa, Y., Yoshioka, K., Matsueda, H., Fujii, K., Dokiya, Y., 2004. Monitoring the SO_2 concentration at the summit of Mt. Fuji and a comparison with other trace gases during winter. J. Geophys. Res. 109, D17304.

Itahashi, S., Hayami, H., 2015. Evaluation of source apportionments from domestic/overseas impacts on sulfate aerosol concentration in Japan on the basis of tagged tracer method in regional chemical transport model. J. Jpn. Soc. Atmos. Environ. 50, 138-151.

Kaneyasu, N., Igarashi, Y., 2007. Light absorption characteristics of atmospheric aerosols observed at the summit of Mt. Fuji in early summer. Earozoru Kenkyu, 22, 318-321.

Kasper, A., Puxbaum, H., 1998. Seasonal variation of SO_2, HNO_3, NH_3 and selected aerosol components at Sonnblick (3106 m a.s.l.). Atmos. Environ. 32, 3925-3939.

Kato S., Shiobara Y., Uchiyama K., Miura K., Okochi H., Kobayashi H., Hatakeyama S., 2016. Atmospheric CO, O_3, and SO_2 measurements at the summit of Mt. Fuji during the summer of 2013. Aerosol Air Qual. Res. 16, 2368-2377.

Kitto A.-M. N., Harrison R. M., 1992. Nitrous and nitric acid measurements at sites in south-east England. Atmos. Environ. 26A, 235-241.

Mitsuishi, K., Iwasaki, M., Takeuchi, M., Okochi, H., Kato, S., Ohira, S., Toda, K., 2018. Diurnal variations in partitioning of atmospheric glyoxal and methylglyoxal between gas and particles at the ground level and in the free troposphere. ACS Earth Space Chem. 2, 915-924.

Murosaki, M., Fujita, S.-I., Takahashi, A., Hayami, H., Miura, K., 2006. Measurements of ozone vertical distribution at Mt. Fuji using a passive sampler. J. Jpn. Soc. Atmos. Environ. 41, 347-354.

Nakazawa, T., Aoki, S., Fukabori, M., Tanaka, M., 1984. The concentration of atmospheric carbon dioxide on the summit of Mt. Fuji (3776 m), Japan. J. Meteorol. Soc. Jpn. 62, 688-695.

Newby, D. E., Mannucci, P. M., Tell, G. S., Baccarelli, A. A., Brook, R. D., Donaldson, K., Forastiere, F., Franchini, M., Franco, O. H., Graham, I., Hoek, G., Hoffmann, B., Hoylaerts, M. F., Künzli, N., Mills, N., Pekkanen, J., Peters, A., Piepoli, M. F., Rajagopalan, S., Storey,R. F., 2015. Expert position paper on air pollution and cardiovascular disease. Eur. Heart J., 36, 83-93.

Okamoto, S., Tanimoto, H., 2016. A review of atmospheric chemistry observations at mountain sites. Prog. in Earth and Planet. Sci. 3, 34.

Preunkert, S., Legrand, M., Jourdain, B., Dombrowski-Etchevers, I., 2007. Acidic gases (HCOOH, CH_3COOH, HNO_3, HCl, and SO_2) and related aerosol species at a high mountain Alpine site (4360 m elevation) in Europe. J. Geophys. Res. 112, D23S12.

Seinfeld, J. H., Pandis S. M., 1998. Atmospheric Chemistry and Physics: From Air Pollution to Climate Change. Wiley-Interscience, New York.

Simon, P. K., Dasgupta, P. K., 1995. Continuous automated measurement of gaseous nitrous and nitric acids and particulate nitrite and nitrate. Environ. Sci. Technol. 29, 1534-1541.

Streets, D. G., Waldhoff, S. T., 2000. Present and future emissions of air pollutants in China: SO_2, NO_x, and CO. Atmos. Environ. 34, 363-374.

Suzuki, I., Hayahi, K., Igarashi, Y., Takahashi, H., Sawa, Y., Ogura, N., Akagi, T., Dokiya, Y., 2008. Seasonal variation of water-soluble ion species in the atmospheric aerosols at the summit of Mt. Fuji. Atmos. Environ. 42, 8027-8035.

Takeuchi M., Izumi M., Watanabe M., Tanaka H., Obata T., Toda K., 2013. Surface modified annular wet denuder for the collection of water-soluble trace gases. Anal. Methods 5, 6071-6075.

Takeuchi M., Li J., Morris K. J., Dasgupta P. K., 2004a. Membrane-based parallel plate denuder for the collection and removal of soluble atmospheric gases. Anal. Chem. 76, 1204-1210.

Takeuchi, M., Miyazaki Y., Tanaka, H., Isobe, T., Okochi, H., Ogata, H., 2017. High time-resolution monitoring of free-tropospheric sulfur dioxide and nitric acid at the summit of Mt. Fuji, Japan. Water Air Soil Pollut. 228, 325.

Takeuchi, M., Miyazaki, Y., Tsunoda, H., Tanaka, H., 2013. Atmospheric acid gases in Tokushima, Japan, monitored with parallel plate wet denuder coupled ion chromatograph. Anal. Sci. 29, 165-168.

Takeuchi M., Namikawa M., Okamoto K., Oda T., Tanaka H., Okochi H., Toda K., Miura K., Tanaka H., 2021. On-line analysis of water-soluble acidic gases and anions in particles at the southeastern foot of Mt. Fuji. Bunseki Kagaku 70, 65-69.

Takeuchi M., Okochi H., Igawa M., 2004b. Characteristics of water-soluble components of atmospheric aerosols in Yokohama and Mt. Oyama, Japan from 1990 to 2001. Atmos. Environ. 38, 4701-4708.

Takeuchi, M., Tsunoda, H., Tanaka, H. and Shiramizu, Y., 2011. Parallel-plate wet denuder coupled ion chromatograph for near-real-time detection of trace acidic gases in clean room air. Anal. Sci. 27, 805-810.

Takeuchi, M., Ullah, S. M. R., Dasgupta P. K., Collins, D. R., Williams, A., 2005. Continuous collection of soluble atmospheric particles with a wetted hydrophilic filter. Anal. Chem. 77, 8031-8040.

Takeuchi, M., Yoshioka, K., Toyama, Y., Kagami, A., Tanaka, H., 2012. On-line measurement of perchlorate in atmospheric aerosol based on ion chromatograph coupled with particle collector and post-column concentrator. Talanta 97, 527-532.

Tsuboi, K., Hosomi, T., Dokiya, Y., Tsutsumi, Y., Yanagisawa, K., Tanaka, S., 1996. Chemical species in aerosol, gases and precipitation at summit of Mt. Fuji. Earozoru Kenkyu 11, 226-234.

Ullah S. M. R., Takeuchi M., Dasgupta P. K., 2006. Versatile gas/particle ion chromatograph. Environ. Sci. Technol. 40, 962-968.

Warneck, P., 1999. Chemistry of the Natural Atmosphere, Vol. 71, 2nd ed., Academic Press , San Diego.

Yokota, K., Nagahuchi, O., Yamane, S., Honda, A., Isezaki, U., 2009. Vertical distribution of gaseous in environmental atmosphere at Mt. Fuji using passive sampler. J. Ecotechnol. Res. 15, 31-36.

Table 1. Ratios of SO_4^{2-} to sum of SO_4^{2-} and NO_3^- concentration, SO_2 to the sum of SO_2 and HNO_3 concentrations, and SO_4^{2-} to SO_2 concentration.

Air parcel	$[SO_4^{2-}]/([SO_4^{2-}] + [NO_3^-])$	$[SO_2]/([SO_2] + [HNO_3])$	$[SO_4^{2-}]/[SO_2]$
A	0.95	0.67	0.60
B	0.95	0.48	2.92
C	0.89	0.54	1.87

Air parcel A, via the Sea of Japan; B, via Russia, northeastern China, and the Korean Peninsula; C, via the East China Sea.

Figure Captions

Fig. 1. Instrument schematic of water-soluble acidic gas/particulate anions monitor.
Abbreviations: AP, air pump; MFC, mass flow controller; WT, water trap; PC, particle collector; PPWD, parallel-plate wet denuder; ATC_1 - ATC_3, anion trap column; PP_1 - PP_3, peristaltic pump; V_1, 3-port valve; V_2, 6-port valve; IC, ion chromatograph; LP, liquid pump; EG, eluent (KOH) generator; CC, concentration column; GC, guard column; SC, separation column; SP, suppressor; CRD, carbonate removal device; CD, conductivity detector; S_1 & S_2, sample bottle; *v*, vent; *w*, waste. The solid and thick dashed lines indicate the liquid and airflows, respectively.

Fig. 2. Temporal variations of water-soluble acidic gases concentration, anions concentration in the particulate matter, abundance ratio of the gaseous compound, and meteorological data during July 10 to 12 in 2016 on the summit of Mt. Fuji, Japan. The shaded regions are the nighttime hours (sunset to sunrise).

Fig. 3. Backward trajectories during the sampling period on the summit of Mt. Fuji, Japan.
The starting times of trajectory were from 09:00 on July 10 to 24:00 on July 12, 2016, at 6 h intervals. The arrow represents the change in the direction of the air parcel flowing into the sampling point (A → B → C).

Fig. 4. Average concentrations of water-soluble acidic gases and particulate anions are classified according to the pattern of air parcel trajectory.
Arrow A, via the Sea of Japan; B, via Russia, northeastern China, and the Korean Peninsula; C, via the East China Sea. The line width of the arrows shows the relative frequency of the entire air parcel trajectory. At the center of the circular graphs, the numerical values show the sum of the concentrations of HNO_3, SO_2, NO_3^-, and SO_4^{2-} in nmol m^{-3}. The area of circular diagrams is proportional to the numerical values.

Fig. 1

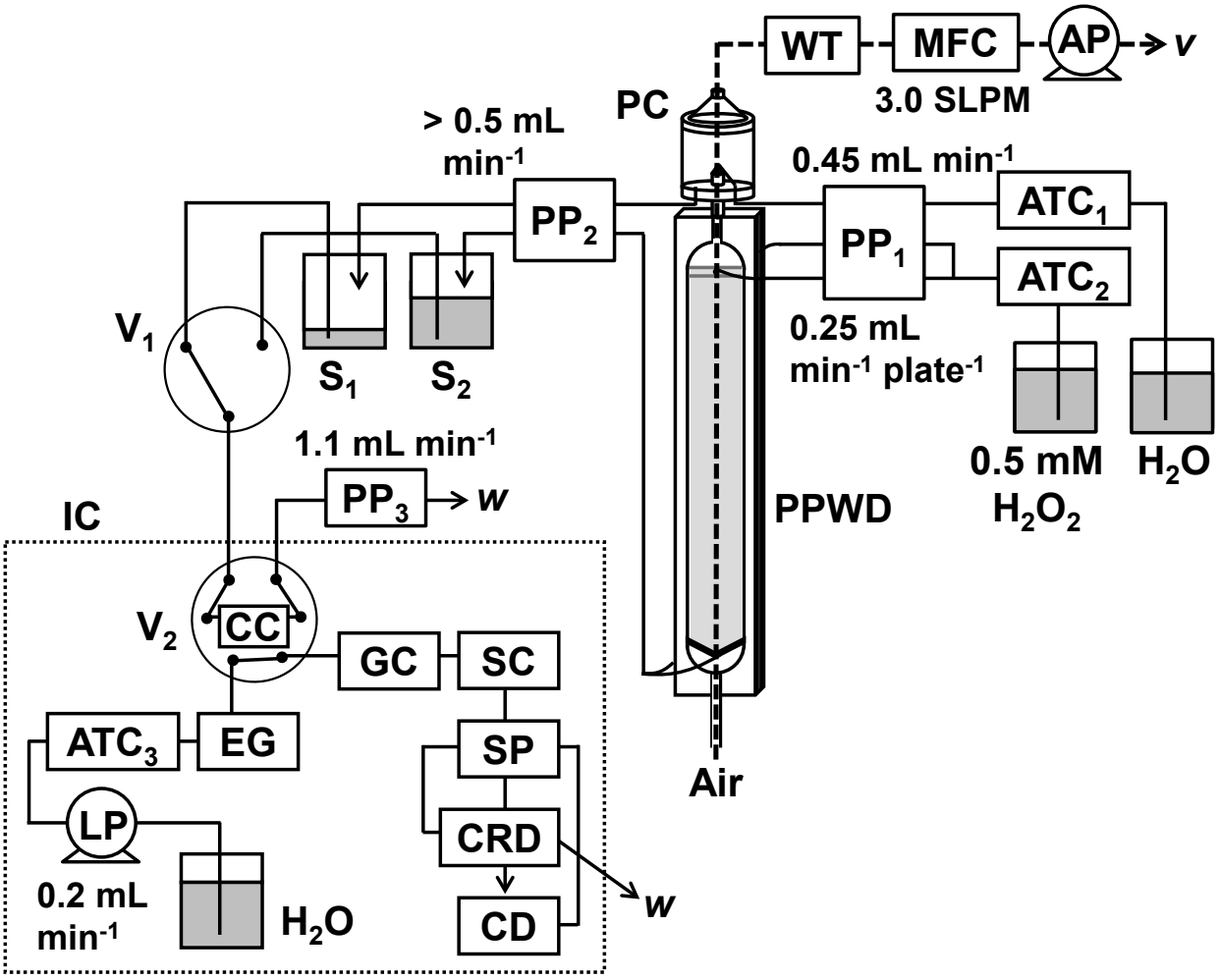
WT
MFC
AP
v
3.0 SLPM
PC
> 0.5 mL min-1
PP2
0.45 mL min-1
ATC1
PP1
ATC2
V1
S1
S2
0.25 mL min-1 plate-1
1.1 mL min-1
PP3
w
IC
PPWD
0.5 mM H2O2
H2O
V2
CC
GC
SC
ATC3
EG
SP
LP
CRD
Air
0.2 mL min-1
H2O
CD
w

Fig. 2

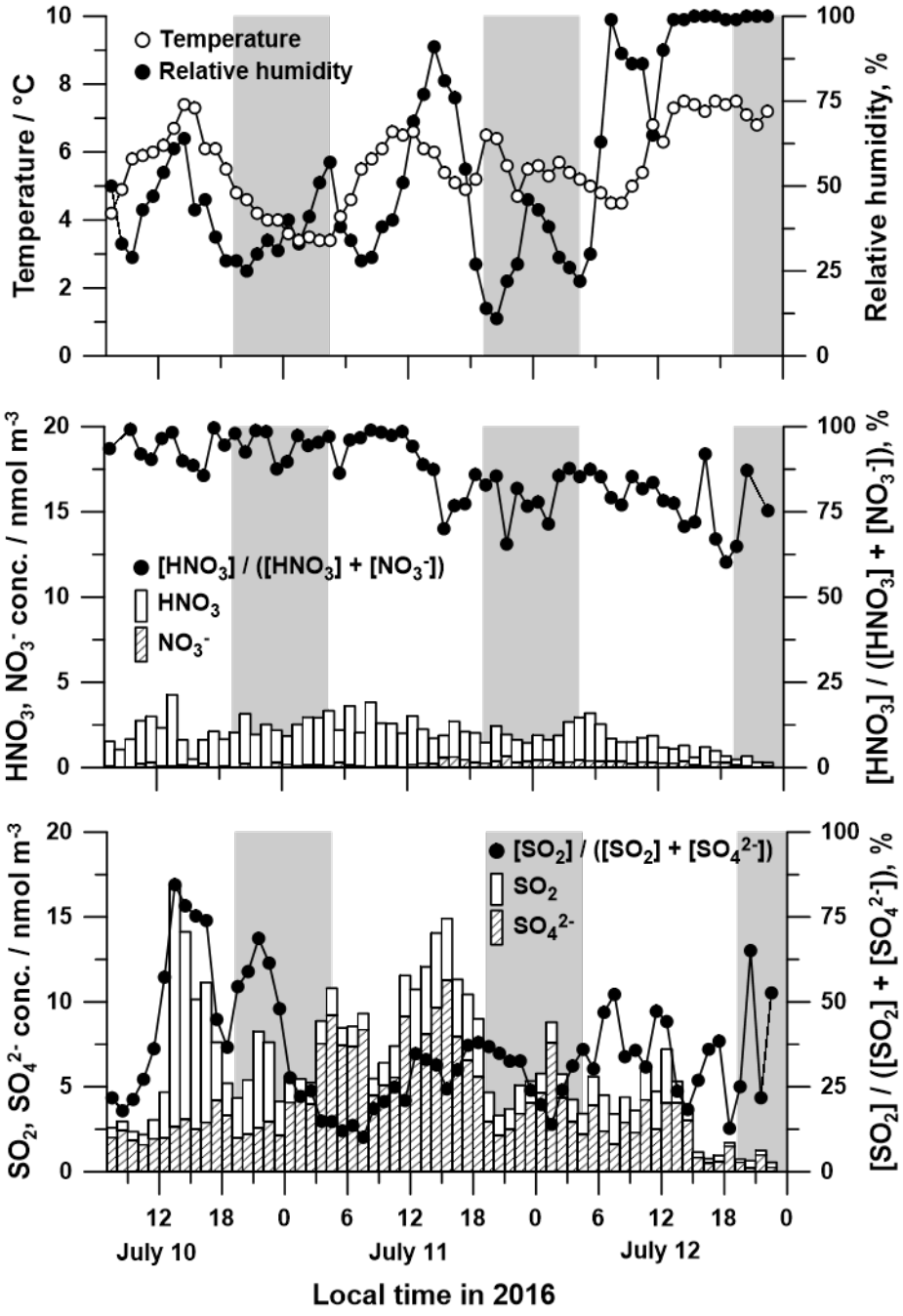
Temperature
Relative humidity
Temperature / °C
Relative humidity, %
[HNO3] / ([HNO3] + [NO3-])
HNO3
NO3-
HNO3, NO3- conc. / nmol m-3
[HNO3] / ([HNO3] + [NO3-]), %
[SO2] / ([SO2] + [SO4 2-])
SO2
SO4 2-
SO2, SO4 2- conc. / nmol m-3
[SO2] / ([SO2] + [SO4 2-]), %
12 18 0 6 12 18 0 6 12 18 0
July 10
July 11
July 12
Local time in 2016

Fig. 3

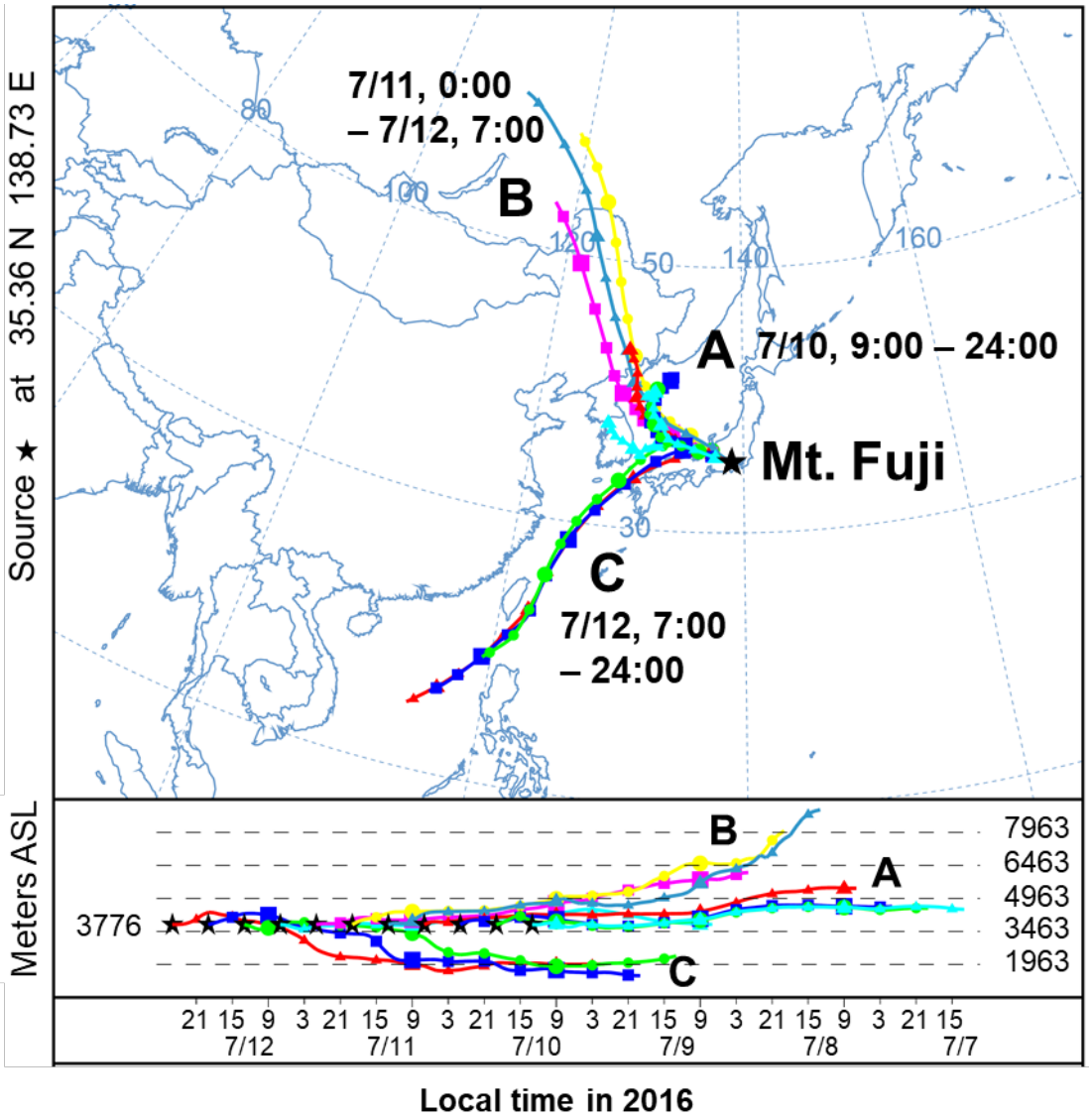
Source ★ at 35.36 N 138.73 E
7/11, 0:00
– 7/12, 7:00
B
A
7/10, 9:00 – 24:00
★ Mt. Fuji
C
7/12, 7:00
– 24:00
80
100
120
50
140
160
30
Meters ASL
3776
7963
6463
4963
3463
1963
21 15 9 3 21 15 9 3 21 15 9 3 21 15 9 3 21 15 9 3 21 15
7/12
7/11
7/10
7/9
7/8
7/7
Local time in 2016

Fig. 4

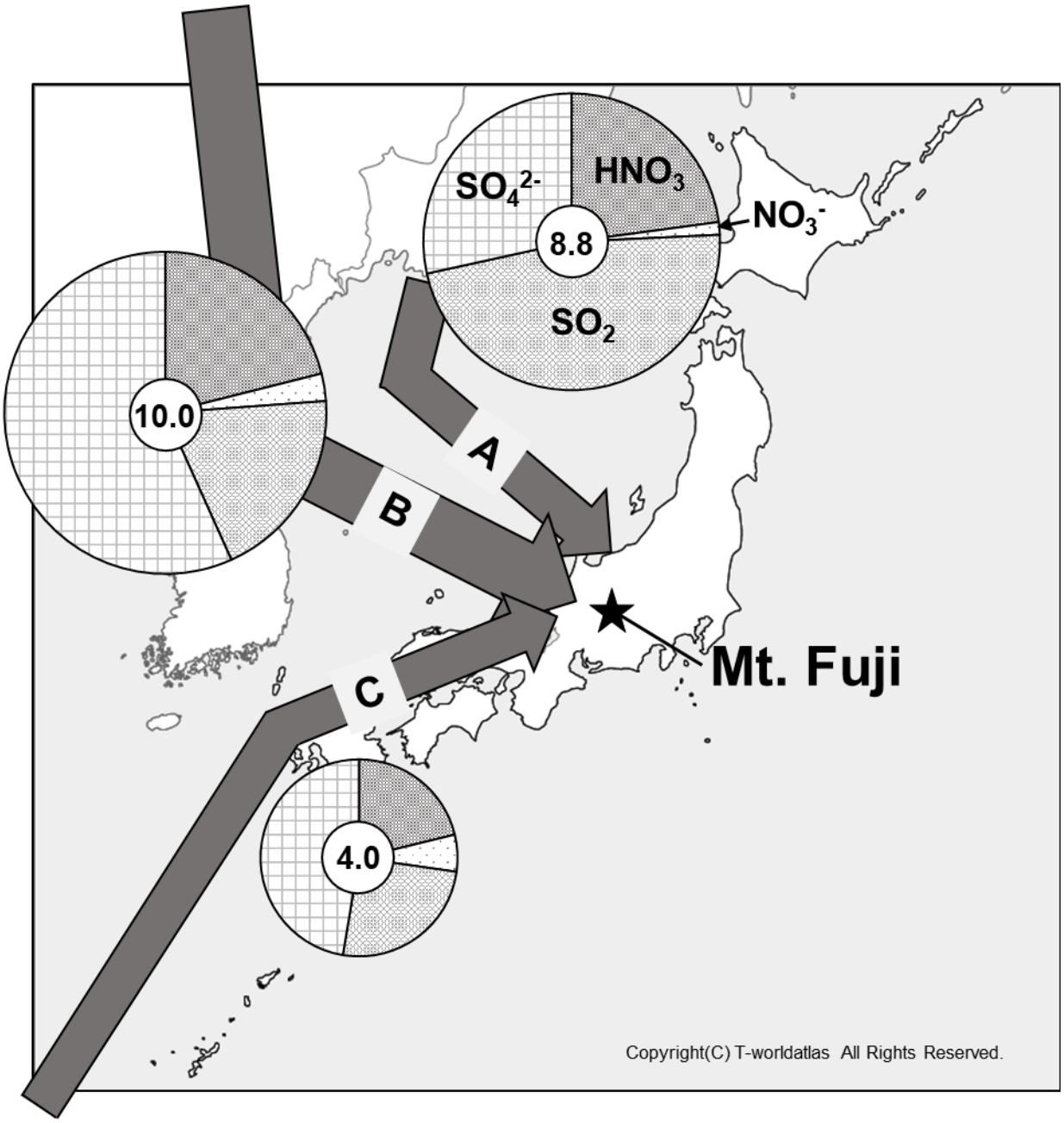
SO_4^{2-}
HNO_3
NO_3^-
8.8
SO_2
10.0
A
B
C
4.0
Mt. Fuji
Copyright(C) T-worldatlas All Rights Reserved.